Measurement of local droplet parameters using single optical fiber probe in the horizontal stratified wavy flow

Byeonggeon Bae [a], Taeho Kim [a], Jae Jun Jeong [a], Kyungdoo Kim [b], Byongjo Yun [a*]
[a]*Department of Mechanical Engineering, Pusan National University, 63 beon-gil 2, Busandaehak-ro, Geumjeong-gu, Busan, 46241*
[b]*Korea Atomic Energy Research Institute, 989 beon-gil, Daedeok-daero, Yuseong-gu, Daejeon, 34057*
[*]*Corresponding author: bjyun@pusan.ac.kr*

1. Introduction

A horizontal stratified wavy flow is observed at the cold-leg and hot-leg pipes in the loss-of-coolant accident (LOCA) of a light water reactor (LWR)-type nuclear power plant. In this flow regime, droplets are entrained from the liquid interfacial wave due to the interfacial shear force caused by high gas velocity [1]. The droplet has a large interfacial area density and therefore has a significant effect on the mass and heat transfer between gas and liquid phases. Therefore, the measurement of local droplet parameters is important for the understanding and modeling of the droplet parameters in the horizontal stratified wavy flow. For this, we applied a stretched conical optical fiber probe (SC-OFP) sensor to measure local droplet parameters such as droplet fraction, droplet velocity, droplet diameter, and droplet mass flux in the horizontal air-water flow. The average droplet mass flow rate along the axial direction of the flow channel was obtained using the local droplet data.

2. Experimental Facility

The experimental facility consists of a water-air injection line, a test section, and the measurement sections for droplet parameters, as shown in Fig. 1. Water and air are supplied by a centrifugal pump with a maximum flow rate of 796 kg/m^{2}s (0.796 m/s) and a roots-type blower with a maximum flow rate of 63.7 kg/m^{2}s (53 m/s), respectively. Water is recirculated through the water tank, and air after passing through the test section is discharged to the atmosphere. The water and air flow rates are measured via a Coriolis flow meter (Micro Motion CMF series) with a maximum uncertainty of 1.99 kg/m^{2}s and a thermal mass flow meter (SAGE) with a maximum uncertainty of 0.78kg/m^{2}s, respectively. The inlet nozzle for the air-water injection into the test section was designed and manufactured by a 3-D printer to make a stratified flow regime since the droplet entrainment is significantly affected by the injection geometry of air-water. Fig. 2 shows the geometry of the inlet nozzle of the test section, which considers a concave liquid-film distribution appeared at a fully developed region of the pipe. This is changed according to the flow conditions. The test section was made of acrylic with a pipe inner diameter of 40 mm and a length of 5.5 m. The SC-OFP sensor was installed at 0.7 m, 2.2 m, 3.2 m, 4.2 m (length-to-diameter ratio=17.5, 55.0, 80.0, and 105.0) from the inlet of the test section. In order to measure the local distribution of droplet parameters, the measurement section with the SC-OFP sensor was equipped with a 1-D traverse system for measurement in the radial direction of the pipe and a rotatable system for measurement in the circumferential direction of the pipe. Fig. 3 shows the dimensions and shape of the SC-OFP sensor fabricated for use in the present experiment. The data obtained from the SC-OFP sensor at each local measurement point was recorded for 60 s at a sampling rate of 4 MHz in the data acquisition system.

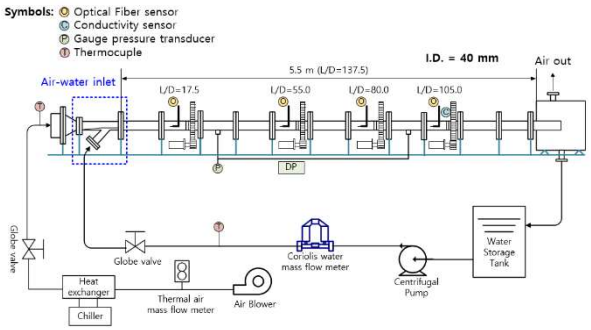

Figure 1. Schematic diagram of experimental facility

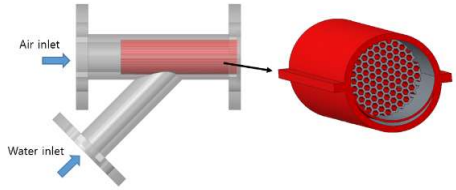

Figure 2. The geometry of air-water injection nozzle

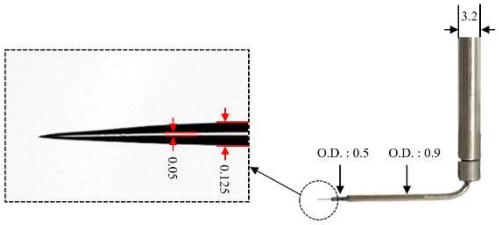

Figure 3. Image of SC-OFP sensor (dimension: mm)

3. Measurement method for droplet parameter

The OFP sensor is based on the principle that the intensity of the light returning to the OFP sensor changes with the refractive index of the medium in contact with the sensor tip after the light reaches the senor tip along the core of the optical fiber. The intensity from the OFP sensor is converted to a voltage difference between the air and water phases. Fig. 4 shows a typical signal

obtained from the SC-OFP sensor. When the droplet pass through the sensor tip, it can be confirmed that the voltage drops rapidly and then returns to the level of the gas phase. At this time, droplet data analysis is performed using the starting and ending points of the droplet passing through the tip of the SC-OFP sensor. These boundary points are determined by peak points of the second-order differential of the droplet signal. The algorithm for this was developed and verified by Kim and Yun et al. [2].

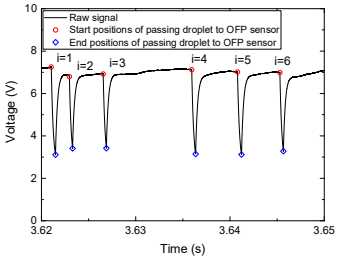

Figure 4. Typical droplet signal obtained from SC-OFP sensor

From the droplet signal, the values for local droplet fraction, droplet velocity, droplet diameter, and droplet mass flux can be obtained. The droplet fraction, α_d, is defined as the ratio of the accumulated residence time taken for the droplet to pass through the tip of the SC-OFP sensor to the total measurement time, as given by Eq. (1).

$$\alpha_d = \frac{\sum_{i=1}^{N} \Delta t_{residence,i}}{T_{total}} \quad (1)$$

The droplet velocity, u_d, is calculated from the signal change rate of the SC-OFP sensor when the droplet passes through the sensor tip. In this regard, Saito et al. [3] proposed a parameter, g_{rd}, defined by Eq. (2) and found that g_{rd} is proportional to the droplet velocity, as given by Eq. (3).

$$g_{rd} = \frac{\Delta V}{\Delta t} \cdot \frac{1}{V_{gas} - V_{liquid}} \quad (2)$$

where $\Delta V/\Delta t$ is the rate of change of the voltage signal from a 90% level to a 70% level from the base signal to the maximum signal output in the droplet signal.

$$u_d = a \cdot g_{rd}^{b} \quad (3)$$

where a and b are the coefficients determined by the calibration test of the SC-OFP sensor for droplet velocity.

Kim and Yun et al. [2] showed that the droplet velocity was affected by $\Delta t_{residence}$ and α_d as well as g_{rd} from calibration data, which was obtained with the help of a high-speed photography method and Laser Doppler Velocimetry (LDV) in the preliminary calibration test. The LDV system has a calibration uncertainty of 0.07 % for velocity. For the determination of droplet velocity, a Neural-Network Training (NNT) method was applied to the calibration data. The uncertainty of droplet velocity predicted by the NNT method using the SC-OFP sensor for the reference droplet velocity is the mean absolute percentage error of 15%.

The droplet diameter, d_d, is determined from the distribution of droplet chordal length, L_d, which is calculated from the product of droplet velocity and residence time in the sensor, as given by Eq. (4).

$$L_d = u_d \cdot \Delta t_{residence} \quad (4)$$

The local droplet mass flux, G_d, is calculated from the local droplet fraction, droplet velocity, and droplet density.

$$G_d = \rho_d u_d \alpha_d \quad (5)$$

The detailed explanations for the measurement methods of the droplet velocity and droplet diameter are described by Kim and Yun et al. [2].

4. Experimental results

The local distributions of droplet parameters, such as droplet fraction, droplet velocity, droplet diameter, and droplet mass flux, were measured at constant j_g=32 m/s according to the change in j_l (0.015, 0.022, and 0.030 m/s), and at constant j_l=0.022 m/s according to the change in j_g (24, 28, and 32 m/s). A horizontal stratified wavy flow was observed at these flow conditions in the present experiment. The temperatures of air and water were maintained at approximately 15℃.

The local measurement positions are five locations along the circumferential direction of the pipe with intervals of 22.5°, from 0° to 90°, and 27 points in the radial direction of the pipe at each circumferential angle, as shown in Fig. 5. The local droplet parameters were measured at 135 points at each axial measurement plane, which corresponded to half of the cross-sectional area of the flow channel. The symmetry of the data with respect to the vertical centerline of the pipe has been confirmed. The local distributions of the droplet parameters were simultaneously measured using SC-OFP sensors installed at four locations along the flow axial direction of the test section.

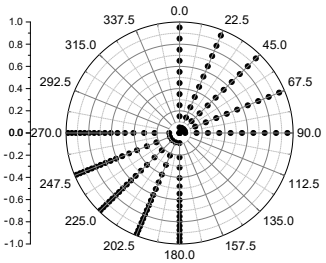

Figure 5. Measurement points in the cross section of the pipe

4.1 Separation of droplet and liquid interfacial wave at the air-water interface

Fig. 6 shows the representative distributions of the fraction of droplet, wave, and total liquid along the vertical centerline of the pipe. In the upper region of the horizontal pipe, all of the liquid is present as a droplet, but the droplet exists with the liquid interfacial wave near

the bottom wall of the pipe. To obtain the local data corresponding to the droplet in the lower region of the pipe, we divided the data of droplets and waves by the critical time difference value. This critical time difference value is defined as the ratio of the maximum droplet diameter, $d_{d,\,max}$, to the wave velocity, u_{wave}.

$$\Delta t_{critical} = \frac{d_{d,max}}{u_{wave}} \tag{6}$$

where $d_{d,\,max}$ is determined as the value when the maximum droplet diameter appearing near the interface in the droplet diameter distribution is constant through iterative calculation. In the present experiment, $d_{d,\,max}$ appeared in the range of 1 mm to 1.5 mm. The droplet velocity is calculated by the correlation of Kumar et al. [4] applicable to vertical, horizontal stratified, and annular flow, as follows,

$$u_{wave} = \frac{\psi j_g + j_l}{1+\psi} \tag{7}$$

where $\psi = 5.5\sqrt{\frac{\rho_g}{\rho_l}}\left(\frac{Re_l}{Re_g}\right)^{0.25}$ and $Re_k = \frac{\rho_k j_k D}{\mu_k}$, k: phase of the gas or liquid.

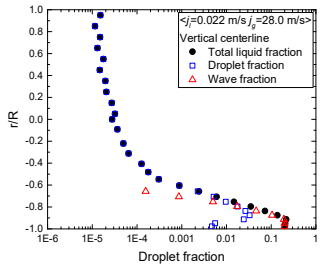

Figure 6. Fraction distributions of the droplet, wave, and total liquid along the vertical centerline of the pipe

To verify the technique for separating droplet and wave signals around the liquid interface wave, a synchronized visualization test was performed using a high-speed camera at 30,000 frames per second (FPS) and an SC-OFP sensor at the air-water interface in a horizontal rectangular channel with a width of 40 mm, a height of 50 mm, and length of 4.2 m. As the side wall of the rectangular channel is flat, visualization is easy compared to the circular pipe. The test was conducted at j_l=0.030 m/s and j_g=24 m/s. The data of the SC-OFP sensor were obtained at a height of 7.5 mm from the center bottom of the flow channel. Fig. 7 shows the results of the synchronization test for the behavior of (a) droplet, (b) wave crest, and (c) liquid filament rupture. From the acquired images, it is possible to determine whether the material in contact with the tip of the SC-OFP sensor is a droplet or a wave. Fig. 8 shows the residence time corresponding to the droplet, wave crest, and filament rupture passing through the sensor tip of the SC-OFP based on the results of the synchronization test. It can be seen that the residence time of the droplet is shorter than that of the wave. The dashed line in Fig. 8 corresponding to the critical time was determined by Eq. (6). The droplets and waves are properly separated based on the critical time, as shown in Fig. 8. On the other hand, the residence time of the filament rupture is shorter than the critical time. This is because the filament rupture accelerates quickly due to the drag force of the high speed gas phase. The thin filament rupture immediately breaks into several droplets and thus the corresponding data can be treated as those of the droplet.

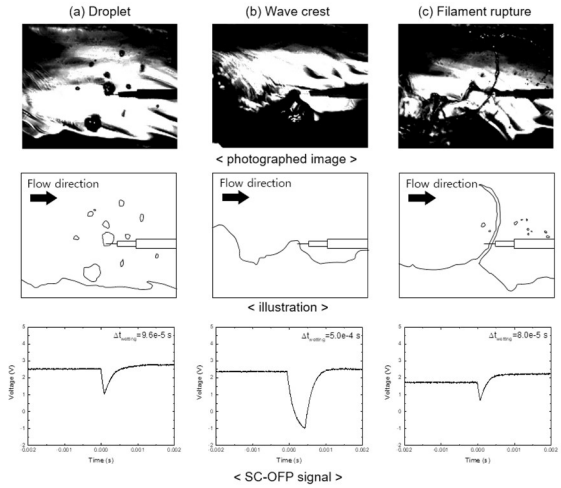

Figure 7. Results of synchronization test using a high-speed camera and an SC-OFP sensor around liquid wave in the horizontal rectangular channel

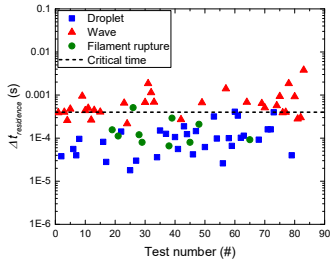

Figure 8. Residence time of droplet, wave, and filament rupture passing through SC-OFP sensor at air-water interface in the horizontal rectangular channel

4.2 Local distribution of droplet parameters on the measuring plane

Fig. 9 shows the typical local distribution of droplet fraction, droplet velocity, droplet diameter, and droplet mass flux in the cross section of the pipe. The black colored data represent the local droplet distribution along the vertical centerline of the pipe and the orange colored data represent the local droplet distribution in the horizontal centerline of the pipe. In the vertical centerline, it can be found that the local droplet fraction and droplet mass flux are much larger near the bottom of the pipe due to gravity effect, and decrease as goes to the top of the pipe. The local droplet diameter is also relatively large in the lower region of the pipe and there are droplets having various sizes at this region. This is because the droplets generated and entrained from the interfacial waves. The local droplet velocity near the bottom of the pipe is small

and then increases toward the top of the pipe. In the gas region, the overall droplet velocity is similar to the gas superficial velocity. As the circumferential angle for measuring local data increases, the asymmetric distribution gradually decreases and the distribution in the horizontal centerline of the pipe is symmetrical.

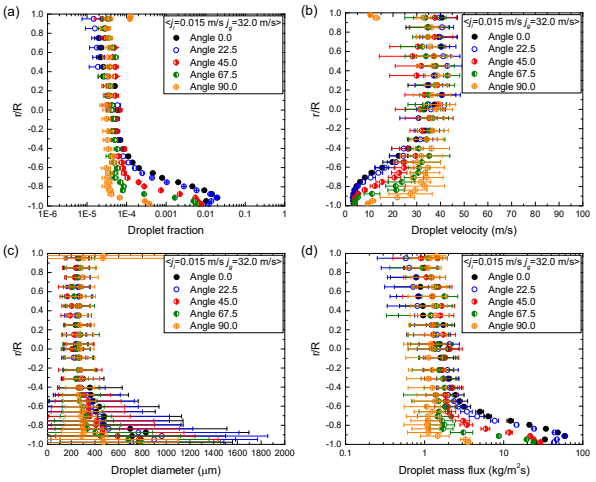

Figure 9. Local distribution of droplet parameters in the cross section of the pipe: (a) droplet fraction, (b) droplet velocity, (c) droplet diameter, (d) droplet mass flux

4.3 Axial droplet mass flow rate along the test section

Fig. 10 shows the droplet mass flow rate measured at four locations with L/D=17.5 (0.7 m), 55.0 (2.2 m), 80.0 (3.2 m), 105.0 (4.2 m) in the flow axial direction of the test section. The average droplet mass flow rate is calculated from the local distributions of droplet fraction and droplet velocity, as follows,

$$m_d = \rho_l \langle u_d \rangle_d \langle \alpha_d \rangle A \tag{8}$$

where

$$\langle u_d \rangle_d = \frac{\langle u_d \alpha_d \rangle}{\langle \alpha_d \rangle} = \frac{\sum_{i=1}^{N} u_{d,i} \alpha_{d,i} \delta A_i}{\sum_{i=1}^{N} \alpha_{d,i} \delta A_i} \tag{9}$$

$$\langle \alpha_d \rangle = \frac{\sum_{i=1}^{N} \alpha_{d,i} \delta A_i}{\sum_{i=1}^{N} \delta A_i} \tag{10}$$

The dotted lines in Fig. 10 were obtained by fitting of corresponding colored data. The droplet mass flow rate at the position of 0.7 m downstream from the inlet of the test section are smaller than that at other positions. From this, it can be seen that the slope of the change of droplet mass flow rate is steep at the inlet of the pipe and then gradually decreases as goes to downstream of the test section. This tendency is explained by the fact that the droplet entrainment rate at the inlet of the flow channel is dominant compared to the droplet deposition rate. Furthermore, the droplet deposition rate increases gradually in proportion to the amount of droplet as goes toward the downstream of the test section. The results of droplet mass flow rate are found to be nearly constant after 3 m downstream from the inlet nozzle in all flow conditions. This implies that the droplet entrainment rate and the droplet deposition rate become equal and the droplet flow is reached to the fully developed condition.

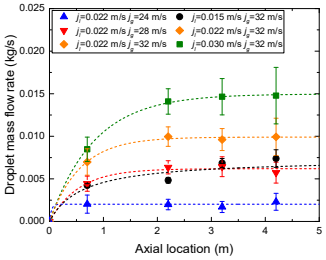

Figure 10. Axial droplet mass flow rate along the test section

3. Conclusions

The local distributions of droplet fraction, droplet velocity, droplet diameter, and droplet mass flux were measured using an SC-OFP sensor at four locations along the flow axial direction of the test section in a horizontal pipe with an inner diameter of 40 mm and a length of 5.5 m. Experimental results showed that the SC-OFP sensor could be applied successfully to the measurement of local droplet parameters for an asymmetric droplet distribution by characteristics of the horizontal stratified flow. The average droplet mass flow rate in the flow axial direction was obtained from the local data. The amount of droplet generated near the inlet of the test section was relatively less, and after 3 m from the inlet of the pipe, the overall data became constant. Through this, it was confirmed that the droplet flow was fully developed. In the further studies, we will develop droplet entrainment depositions models by using present experimental data.

Acknowledgement

This work was supported by the Nuclear Research & Development Program of the NRF (National Research Foundation of Korea) grant funded by the MSIP (Ministry of Science, ICT and Future Planning), Republic of Korea and funded by Korea Hydro & Nuclear Power Co., LTD. (Grant code: NRF-2017M2A8A4015059).

REFERENCES

[1] Bae, B., Ahn, T., Jeong, J., Kim, K., and Yun, B., Characteristics of an interfacial wave in a horizontal air-water stratified flow, International Journal of Multiphase Flow, Vol.97, p.197-205, 2017.
[2] Kim, T., Ahn, T., Bae, B., Jeong, J., Kim, K., and Yun, B., Measuring local droplet parameters using single optical fiber probe, AIChE journal, 2019, http://doi.org/10.1002/aic.16591 .
[3] Saito, T., Matsuda, K., Ozawa, Y., Oishi, S., and Aoshima, S., Measurement of tiny droplets using a newly developed optical fibre probe micro-fabricated by a femtosecond pulse laser, Measurement Science and Technology, 20(11), (2009) 114002.
[4] Kumar, R., Gottmann, M., and Sridhar, K. R., Film thickness and wave velocity measurements in a vertical duct, Journal of fluids engineering, 124(3), (2002) 634-642.